

DESY-99-075
 Edinburgh 6/99
 OUTP-99-27P
 UTCCP-P-67

Precision computation of the strange quark's mass in quenched QCD

Joyce Garden^a, Jochen Heitger^b, Rainer Sommer^b and Hartmut Wittig^{c,d,1}

(ALPHA and UKQCD Collaborations)

^a Department of Physics & Astronomy, University of Edinburgh
 Edinburgh EH9 3JZ, Scotland

^b DESY-Zeuthen
 Platanenallee 6, D-15738 Zeuthen, Germany

^c Theoretical Physics, University of Oxford
 1 Keble Road, Oxford OX1 3NP, UK

^d Center for Computational Physics, University of Tsukuba
 Tsukuba, Ibaraki 305-8571, Japan

Abstract

We determine the renormalization group invariant quark mass corresponding to the sum of the strange and the average light quark mass in the quenched approximation of QCD, using as essential input the mass of the K-mesons. In the continuum limit we find $(M_s + \hat{M})/F_K = 0.874(29)$, which includes systematic errors. Translating this non-perturbative result into the running quark masses in the $\overline{\text{MS}}$ -scheme at $\mu = 2 \text{ GeV}$ and using the quark mass ratios from chiral perturbation theory, we obtain $\overline{m}_s(2 \text{ GeV}) = 97(4) \text{ MeV}$. With the help of recent results by the CP-PACS Collaboration, we estimate that a 10% higher value would be obtained if one replaced F_K by the nucleon mass to set the scale. This is a typical ambiguity in the quenched approximation.

June 1999

¹PPARC Advanced Fellow

1 Introduction

Quark masses are fundamental parameters of the standard model, which have to be determined from experimental observations confronted with theoretical predictions [1]. At present the most precise theoretical predictions which allow for the determination of ratios of the three light quark masses are based on chiral perturbation theory [2]. A detailed analysis yielded [3]

$$M_u/M_d = 0.55 \pm 0.04, \quad M_s/\hat{M} = 24.4 \pm 1.5 \quad (1.1)$$

with

$$\hat{M} = \frac{1}{2}(M_u + M_d). \quad (1.2)$$

Unlike these ratios, the overall magnitude of the quark masses is not accessible to chiral perturbation theory combined with experimental data alone. One should therefore determine a particular linear combination of quark masses by comparing lattice QCD predictions [4–16] or QCD sum rules [17–27] to experiments.

In this work we use the masses of the K-mesons and a computation in the quenched approximation to QCD to determine $M_s + \hat{M}$. Our analysis employs the $O(a)$ improved lattice theory, the quark mass is renormalized completely non-perturbatively [28] and the continuum limit is taken (with a rate proportional to a^2). Hence, with respect to the last two points, it improves on many previous calculations.

In general quark masses are scale- and scheme dependent quantities. It is therefore desirable to compute the *renormalization group invariant quark masses*, which – being both scale- and scheme-independent – are naturally taken as fundamental parameters of QCD. We recall that they are defined in terms of the high energy behaviour of the running masses $\bar{m}(\mu)$:

$$M_i \equiv \lim_{\mu \rightarrow \infty} \left\{ (2b_0\bar{g}^2(\mu))^{-d_0/2b_0} \bar{m}_i(\mu) \right\}, \quad (1.3)$$

$$b_0 = 11/(4\pi)^2, \quad d_0 = 8/(4\pi)^2. \quad (1.4)$$

On the other hand, the renormalization group invariant masses M_i are related to the bare current quark masses m_i by

$$M_i = Z_M m_i \quad (1.5)$$

with a (flavour independent) renormalization factor Z_M which was recently computed by the ALPHA Collaboration [28, 29]. This non-perturbative result is the basis of our present calculation.² The renormalization problem and its solution were discussed in

²Since the bare mass is involved, Z_M depends on the regularization. The complete calculation of [28] was done in $O(a)$ improved lattice QCD, which we use here as well.

detail in references [28, 29]. The current quark masses themselves, are defined through the PCAC relation,

$$\partial_\mu A_\mu(x) = (m_i + m_j)P(x), \quad (1.6)$$

in terms of the axial current,

$$A_\mu(x) = \bar{\psi}_i(x)\gamma_\mu\gamma_5\psi_j(x), \quad (1.7)$$

and the pseudoscalar density,

$$P(x) = \bar{\psi}_i(x)\gamma_5\psi_j(x). \quad (1.8)$$

Applied to the vacuum-to-K matrix elements it reads

$$M_s + \hat{M} = Z_M(m_s + \hat{m}) = Z_M \frac{F_K}{G_K} m_K^2, \quad (1.9)$$

where F_K is the K-meson decay constant, and G_K denotes the vacuum-to-K matrix element of the pseudoscalar density.³ Eq. (1.9) is the fundamental relation which we shall exploit in this work. It is used in the following way: we compute $Z_M \frac{F_K}{G_K}$ and multiply with the experimental squared mass,

$$m_K^2 = \frac{1}{2}(m_{K^+}^2 + m_{K^0}^2)_{\text{QCD}} = (495 \text{ MeV})^2, \quad (1.10)$$

to obtain $M_s + \hat{M}$. By the subscript “QCD” we indicate that we have used the masses in pure QCD with electromagnetic interactions switched off, since obviously the lattice QCD result is valid for a world where $\alpha_{\text{em}} = 0$. In practice this is achieved by subtracting an estimate of the electromagnetic effects from the experimental numbers. The numerical estimate in eq. (1.10) was obtained from Dashen’s theorem [30] being well aware that the accuracy of this estimate may be only around 0.5% in m_K^2 [31].

The combination $Z_M \frac{F_K}{G_K}$ carries the dimension of an inverse mass. Therefore it is necessary to choose another dimensionful observable to form a dimensionless ratio which has a continuum limit (this is often called “setting the scale”). Choosing r_0 [32] or F_K for this second observable and extrapolating to the continuum limit yields the results quoted in the abstract.

In the following we shall first explain our strategy to deal with some technical difficulties in the computation of F_K/G_K . Since it involves a computation of the ratio $F_{\text{PS}}/G_{\text{PS}}$ for mass-degenerate mesons, we discuss in Sect. 3 the dependence of various observables on the difference of quark masses $m_i - m_j$. In Sect. 4 we show that finite size effects are negligibly small in our calculation. The main result for the quark mass is presented in Sect. 5, where, among other issues, the extrapolations to the continuum are discussed. We then proceed to estimate the *ambiguity* which originates from the

³Our convention is that F_K, G_K denote the matrix elements of the bare operators. Renormalization factors are written explicitly. For the $O(a)$ improved lattice theory they can be found in the appendix.

fact that the *quenched approximation* can not be expected to describe the real world properly. As a byproduct, we present the calculation of the kaon decay constant and masses in the vector channel in the continuum limit. We finish with a discussion of our results and some comments on how the method may be extended to determine coefficients of the chiral Lagrangian.

2 Strategy

2.1 Chiral perturbation theory

Let us first recall what chiral perturbation theory can predict concerning the quark masses [2,3,33,34]. Chiral perturbation theory is based on nothing but the very general assumption that chiral symmetry is broken spontaneously in the limit $\hat{M} = M_s \rightarrow 0$. This allows for a quantitative description of the pseudoscalar sector in terms of a low-energy effective Lagrangian, where quark masses appear as “kinematical variables” just like the energy in scattering processes. The parameters in the chiral Lagrangian are independent of the quark masses. At order p^4 , most of the parameters have been determined by comparison to experimental data (see e.g. [35] for numerical values). However, the coefficient of the chiral symmetry breaking quark mass term in the Lagrangian (denoted by B in [34]), cannot be determined from experimental data alone. It can only be fixed when one particular quark mass is known. Since all parameters are independent of the quark masses, this may be done at a convenient reference point. It is important to realize that this reference point does not have to correspond to a physical quark mass. The procedure can then be extended to determine other parameters in the chiral Lagrangian more precisely, once additional observables are known for suitable quark masses and with sufficient accuracy. All of this can potentially be achieved by lattice QCD calculations and can improve predictions such as eq. (1.1). Also the justification for the truncation of chiral perturbation theory can and should, of course, be checked.

A particularly convenient way of applying this idea in practice is as follows. We introduce the ratio

$$R(m_i, m_j) = \frac{F_{\text{PS}}}{G_{\text{PS}}}, \quad (2.1)$$

such that

$$m_i + m_j = R(m_i, m_j) m_{\text{PS}}^2(m_i, m_j). \quad (2.2)$$

Defining a reference quark mass

$$m_{\text{PS}}(m_{\text{ref}}, m_{\text{ref}}) = m_K, \quad (2.3)$$

with the kaon mass already discussed in the introduction, the ratio R for the physical quark masses may be written as

$$R(m_i, m_j) = T(x_i, x_j) R(m_{\text{ref}}, m_{\text{ref}}), \quad x_i = m_i/m_{\text{ref}} \quad (2.4)$$

with a function $T(x_i, x_j)$ which can be computed in chiral perturbation theory. In particular, using [33, 35] one finds

$$T(m_s/m_{\text{ref}}, \hat{m}/m_{\text{ref}}) \approx 1 \quad \text{and thus} \quad 2m_{\text{ref}} \approx m_s + \hat{m}. \quad (2.5)$$

The corrections to the above equation are small, but the overall uncertainties associated with this statement require a detailed investigation of the phenomenology. The reason is that the errors of the parameters in the chiral Lagrangian are correlated, which makes it non-trivial to estimate uncertainties. Nevertheless we expect eq. (2.5) to be correct to within about 10%.

In Sect. 3 we shall follow a complementary approach, by investigating pseudoscalar meson observables as a function of the average quark mass and the difference of the quark masses. We find that the dependence on the latter variable is rather small. It then follows trivially from our definition of T that eq. (2.5) is valid rather precisely.

Before turning to that investigation let us briefly explain why our strategy is advantageous. The reasons for quenched QCD and full QCD are somewhat different but related, having both to do with the difficulties of extrapolations to the region of small quark masses which is at present inaccessible to direct Monte Carlo calculations.

2.2 Quenched approximation and full QCD

The lattice calculations presented in this paper have been performed in the $O(a)$ improved theory [36] with non-perturbative improvement coefficients [37] and mass-renormalization factor, Z_M [28]. Details pertaining to, for instance, $O(a)$ correction terms in the currents can be found in the appendix.

To motivate our strategy let us first review the straightforward approach for computing light quark masses. First one assumes isospin symmetry of the ratios R , i.e. effects of $O(m_u - m_d)$ are neglected, which is well justified given the smallness of this mass difference. Then one chooses an overall scale, say the hadronic radius r_0 , and determines the bare light quark mass and strange quark mass such that $r_0 m_\pi$ and $r_0 m_K$ agree with the experimental numbers. Except for the bare coupling, all parameters in the QCD Lagrangian are then fixed and the current quark masses are given by eqs. (2.1, 2.2), with

$$\langle 0 | A_\mu(0) | K(p) \rangle = i p_\mu F_K, \quad \langle 0 | P(0) | K(p) \rangle = G_K. \quad (2.6)$$

Here $|K(p)\rangle$ denotes a pseudoscalar state with momentum p , standard infinite volume normalization and the proper flavour quantum numbers. After renormalization the quark masses can be extrapolated to the continuum.

While this approach will ultimately be a clean and straightforward way to determine the quark masses, it poses two problems in the quenched approximation.

- The quenched approximation is expected to be misleading for very light quark masses such as \hat{m} . A particular indication of the failure of the quenched approxi-

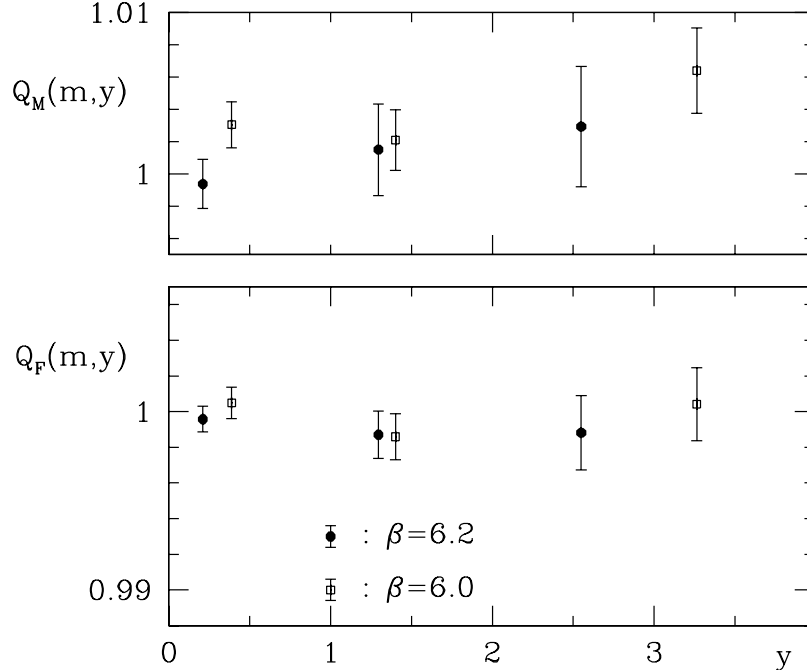


Figure 1: The functions $Q(m, y)$. Q_M denotes the case of pseudoscalar masses and Q_F their decay constants. The average of m_i and m_j is between $\approx 1.4 m_{\text{ref}}$ and $\approx 2.4 m_{\text{ref}}$.

mation in this regime is the presence of logarithmic terms in chiral perturbation theory which have no counterpart in the full theory [38–40].

- With our fermion action and lattice spacings, we cannot perform calculations for quark masses which are below approximately half of the strange quark mass. For smaller masses, the Dirac operator has unphysical zero modes on a certain fraction of configurations contributing to the path integral (“exceptional configuration”) [37, 41].

The second problem is of a more technical nature. It can in principle be circumvented by choosing a suitable action, but then also Z_M has to be recomputed. However, the first point must be taken seriously, since we want to obtain results which are not misleading with respect to the real theory of interest, full QCD.

It is furthermore advantageous to use the same strategy in full QCD. The reason is that it is very likely that for some time to come, lattice simulations will only reach down to quark masses somewhere around $m = m_{\text{ref}} (\approx m_s/2)$. The most precise way to extrapolate further is then given by chiral perturbation theory as discussed above.

3 Non-degenerate quarks

In this section we investigate quantitatively how the pseudoscalar mass and decay constant depend on the difference of the two quark masses in quenched QCD. Apart from

some consistency checks which were performed with the data of the ALPHA Collaboration, the numerical results presented here were obtained during the course of the UKQCD simulations [42] using the $O(a)$ improved action.

We consider the observables of interest as a function of the average current quark mass $m = \frac{m_i + m_j}{2}$ and the parameter y defined by

$$y = (x_i - x_j)^2 = (m_i - m_j)^2 / m_{\text{ref}}^2, \quad (3.1)$$

with m_{ref} as determined later in Sect. 5. In particular, we want to show that the functions

$$H_{\text{M}}(m, y) = m_{\text{PS}}^2 \quad \text{and} \quad H_{\text{F}}(m, y) = F_{\text{PS}} [1 + b_{\text{A}} a m_{\text{q}}] \quad (3.2)$$

have little dependence on y . In other words, the ratios

$$Q_{\text{M}}(m, y) = H_{\text{M}}(m, y) / H_{\text{M}}(m, 0), \quad (3.3)$$

$$Q_{\text{F}}(m, y) = H_{\text{F}}(m, y) / H_{\text{F}}(m, 0), \quad (3.4)$$

are close to unity. Note that the two functions Q_{M} and T are equivalent at the special point $m = m_{\text{ref}}$, since $Q_{\text{M}}(m_{\text{ref}}, y) = 1/T(1 + \frac{1}{2}\sqrt{y}, 1 - \frac{1}{2}\sqrt{y})$. In order to investigate the y -dependence numerically, we start from the results for $a m_{\text{PS}}$ and $a F_{\text{PS}}$ of UKQCD [42] for three values of the quark masses at each of the two bare couplings $\beta = 6.0, 6.2$. Three combinations with $m_j \neq m_i$ are then available for each of the two corresponding lattice spacings, 0.09 fm and 0.07 fm. The only numerical difficulty in examining the ratios Q_X is that the denominators $H_X(m, 0)$ are in general not available directly. They may, however, be replaced by an interpolation

$$H_{\text{M}}(m, 0) = h_1^{\text{M}} m + h_2^{\text{M}} m^2 + h_3^{\text{M}} m^3, \quad (3.5)$$

$$H_{\text{F}}(m, 0) = h_0^{\text{F}} + h_1^{\text{F}} m + h_2^{\text{F}} m^2, \quad (3.6)$$

with h_k^X determined from the observables computed for the three available degenerate mesons ($m_i = m_j$). One has to check that these interpolations are stable. This was tested by taking different subsets of three mass points of the data in Table 1, extracting h_k^X and comparing the resulting functions $H_X(m, 0)$. Deviations between these different interpolations were found to be negligible compared to the statistical precision of the ratios Q themselves.

Before discussing the results, let us mention one technical point in the numerical analysis. For convenience, the above procedure was carried out using the subtracted, improved bare quark masses, $\tilde{m}_{\text{q}} = m_{\text{q}}(1 + b_{\text{m}} a m_{\text{q}})$, $m_{\text{q}} = m_0 - m_{\text{c}}$, instead of the current quark masses themselves.⁴ For the question addressed in this section, this makes no difference because $m = Z_{\text{m}} \tilde{m}_{\text{q}}$ holds up to the usual $O(a^2)$ errors, with some mass-independent renormalization factor Z_{m} .

⁴Flavour indices are suppressed, here, and we use $b_{\text{m}} = -1/2 - 0.0962g_0^2$.

β	κ	am	am_{PS}	am_{V}	aF_{PS}	$\frac{F_{\text{PS}}}{aG_{\text{PS}}}$
6.0	0.1335	0.0466(1)	0.3884(10)	0.5289(26)	0.0969(4)	0.5997(31)
	0.1338	0.03856(6)	0.3529(11)	0.5077(31)	0.0943(4)	0.6022(34)
	0.1340	0.03311(7)	0.3275(11)	0.4938(36)	0.0924(4)	0.6015(39)
	0.1342	0.02759(8)	0.3001(12)	0.4804(44)	0.0905(4)	0.5978(45)
6.1	0.1342	0.04161(3)	0.3306(5)	0.4542(17)	0.0870(3)	0.7454(22)
	0.1345	0.03305(3)	0.2947(5)	0.4328(23)	0.0841(3)	0.7476(26)
	0.1347	0.02734(3)	0.2687(6)	0.4188(28)	0.0820(3)	0.7458(30)
	0.1349	0.02160(4)	0.2399(7)	0.4056(39)	0.0799(3)	0.7405(37)
6.2	0.1347	0.03241(3)	0.2683(5)	0.3748(21)	0.0743(3)	0.8887(33)
	0.1349	0.02661(3)	0.2430(6)	0.3588(26)	0.0721(3)	0.8908(38)
	0.13515	0.01934(3)	0.2080(6)	0.3388(39)	0.0693(3)	0.8857(48)
	0.1352	0.01788(3)	0.2004(6)	0.3348(43)	0.0687(3)	0.8830(51)
6.45	0.13485	0.02477(2)	0.1975(8)	0.2749(25)	0.0533(5)	1.261(10)
	0.1351	0.01734(2)	0.1650(9)	0.2558(37)	0.0503(4)	1.265(14)
	0.1352	0.01439(2)	0.1505(9)	0.2480(46)	0.0490(4)	1.261(16)
	0.1353	0.01142(2)	0.1347(10)	0.2398(59)	0.0477(4)	1.250(19)

Table 1: Results for masses and unrenormalized (ratios of) matrix elements in all simulation points

In Fig. 1 we show our numerical results.⁵ They show that Q_{M} has a dependence on y which is below the level of a percent, and Q_{F} is seen to be independent of y to within our statistical precision of around 0.3%. It should be kept in mind that Fig. 1 tests the y -dependence for $m/m_{\text{ref}} = 1.4\text{--}2.4$, while later we shall be interested in kaon physics, where $m/m_{\text{ref}} \approx 1$. It remains a (plausible!) hypothesis that Q_X are close to unity also for this lower value of m . Nevertheless, our investigation quantifies the smallness of y -effects for the first time and suggests that the correction terms in eq. (2.5) are negligible. Based on this analysis we shall not distinguish between $2m_{\text{ref}}$ and $m_s + \hat{m}$ from now on.

4 Finite size effects

Our numerical results, which are listed in Table 1, have been obtained for approximately constant physical volume, $T \times L^3$, where $T = 2L$ and $L \approx 3r_0 = 1.5\text{fm}$. We used exactly the numerical methods described in [43], and in particular systematic errors due to

⁵The numerical values for $(\tilde{m}_{\text{q}})_{\text{ref}}$ were taken from the analysis described in Sect. 5.

excited state contributions were checked to be small compared to the statistical errors. Further details about the simulation are described in the appendix. Since the precision of the results is quite good one has to investigate whether they may be affected by the finite size of the system at the level of their statistical accuracy. The most relevant observable for the determination of the quark masses is the ratio $R = (m_i + m_j)/m_{\text{PS}}^2$. Since m_i is defined through the PCAC relation, it is independent of the volume [36] (apart from small lattice artefacts of order a^2). We are therefore predominantly interested in the volume dependence of the pseudoscalar masses but will also consider the decay constant F_{PS} .

In the pseudoscalar sector the leading finite size effects can be reliably calculated in chiral perturbation theory. The reason is that for vanishing quark masses the pseudoscalar mesons are Goldstone bosons. Their interactions become weak for small energies and these are responsible for the leading finite size effects for large but finite volumes.

Gasser and Leutwyler have reported results for the two-point function of the axial current at space-like separations [44]. This result, given for finite temperature and in finite volume is easily adapted to the situation which is of interest here, namely the pseudoscalar mass on an L^3 -torus (temperature zero) $m_{\text{PS}}(L)$, and the corresponding decay constant $F_{\text{PS}}(L)$. The resulting formulae are

$$\frac{m_{\text{PS}}(L)}{m_{\text{PS}}(\infty)} - 1 = \frac{1}{N_f} \frac{m_{\text{PS}}^2}{F_{\text{PS}}^2} g(z) + \mathcal{O}(e^{-\sqrt{2}z}), \quad z = m_{\text{PS}} L \quad (4.1)$$

$$\frac{F_{\text{PS}}(L)}{F_{\text{PS}}(\infty)} - 1 = -N_f \frac{m_{\text{PS}}^2}{F_{\text{PS}}^2} g(z) + \mathcal{O}(e^{-\sqrt{2}z}), \quad (4.2)$$

$$g(z) = \frac{3}{8\pi^2 z^2} \int_0^\infty \frac{dx}{x^2} e^{-z^2 x - 1/(4x)} = \frac{3}{2\pi^2 z} K_1(z), \quad (4.3)$$

where $K_1(z)$ denotes a modified Bessel function. Here a comment is in order. This is a result of the first non-trivial order in chiral perturbation theory in full QCD. A priori one cannot expect it to be accurate if the pseudoscalar meson masses are too large. On the other hand, one knows that the finite size effects discussed here are of order e^{-z} , as long as the pseudoscalar is the lightest particle in the theory [45,46]. It is plausible that the prefactor of the exponential is not dramatically different for heavier pseudoscalar mesons. We may therefore take the above equations as a reasonable estimate of finite size effects. Being interested in the order of magnitude of these effects, we also do not worry about the difference of the quenched approximation and full QCD.

In our numerical calculations (see Tables 1 and 4), we are in the range $z = m_{\text{PS}}L \geq 4.3$ and consequently eqs. (4.1)–(4.2) predict corrections which are below the level of 0.5% for F_{PS} and 0.1% for m_{PS} . In order to check this estimate, we have done some calculations on lattices which are larger than our standard $L \approx 1.5$ fm. Entirely consistent with the above formulae, we found no significant changes in $F_{\text{PS}}, m_{\text{PS}}$, for instance

$r_0^2 m_{\text{PS}}^2$	β	$Z_M \frac{R}{r_0}$	$\frac{M_s + \hat{M}}{(F_{\text{PS}})_R}$	$r_0 (F_{\text{PS}})_R$	$m_V r_0$	$\frac{(F_{\text{PS}})_R}{m_V}$
1.5736	6.0	0.1939(30)	0.810(11)	0.3746(45)	2.428(32)	0.1543(26)
	6.1	0.2077(28)	0.824(10)	0.3952(47)	2.457(32)	0.1609(26)
	6.2	0.2160(30)	0.843(11)	0.4020(48)	2.361(40)	0.1701(32)
	6.45	0.2205(46)	0.851(19)	0.4070(60)	2.441(71)	0.1667(52)
	<i>CL</i>	<i>0.2300(69)</i>	<i>0.874(27)</i>	<i>0.4146(94)</i>	<i>2.386(66)</i>	<i>0.1761(75)</i>
3.0	6.0	0.1966(26)	1.450(17)	0.4063(47)	2.637(22)	0.1541(20)
	6.1	0.2104(26)	1.471(17)	0.4288(49)	2.666(20)	0.1609(20)
	6.2	0.2181(28)	1.501(18)	0.4363(51)	2.606(25)	0.1675(23)
	6.45	0.2236(37)	1.518(28)	0.4421(62)	2.677(42)	0.1652(32)
	<i>CL</i>	<i>0.2324(57)</i>	<i>1.553(42)</i>	<i>0.4507(99)</i>	<i>2.645(41)</i>	<i>0.1709(49)</i>

Table 2: Extra-/interpolations in $r_0^2 m_{\text{PS}}^2$ and resulting continuum limits (CL) including all errors

$$\beta = 6.2, am_{\text{PS}} = 0.208 : \quad \frac{m_{\text{PS}}(24a)}{m_{\text{PS}}(32a)} - 1 = 0.003(4) \quad (\approx 0.0009), \quad (4.4)$$

$$\frac{F_{\text{PS}}(24a)}{F_{\text{PS}}(32a)} - 1 = -0.003(8) \quad (\approx -0.003), \quad (4.5)$$

where the numbers in parentheses are the estimates from the above equations with $N_f = 2$.

We conclude that even with the numerical precision of Table 1, finite size effects are negligible for the quark masses considered. Of course, as described by the above formulae, finite size effects grow rapidly when the pseudoscalar mass becomes smaller and larger volumes would be necessary for quark masses which are significantly smaller than the ones we used.

5 Degenerate quarks, continuum limit

We can now proceed to compute the desired quantity $r_0(M_s + \hat{M})$. The first step is to evaluate R for degenerate quarks as a function of $r_0^2 m_{\text{PS}}^2$. Relegating all details of the exact numerical procedure, such as the definition of m_q and the different improvement coefficients, to the appendix we directly show the mass dependence of R in Fig. 2a. It is apparent that R is almost constant as a function of the quark mass (or $r_0^2 m_{\text{PS}}^2$). It is therefore easy to extrapolate to the desired point $r_0^2 m_{\text{PS}}^2 = r_0^2 m_{\text{K}}^2 = 1.5736$, slightly outside of the range where we have numerical results. The extrapolation is performed linearly in $r_0^2 m_{\text{PS}}^2$, using the three closest data points. Simply taking for instance the closest data point or an average of all of them would change the final result for the quark mass by a negligible amount.

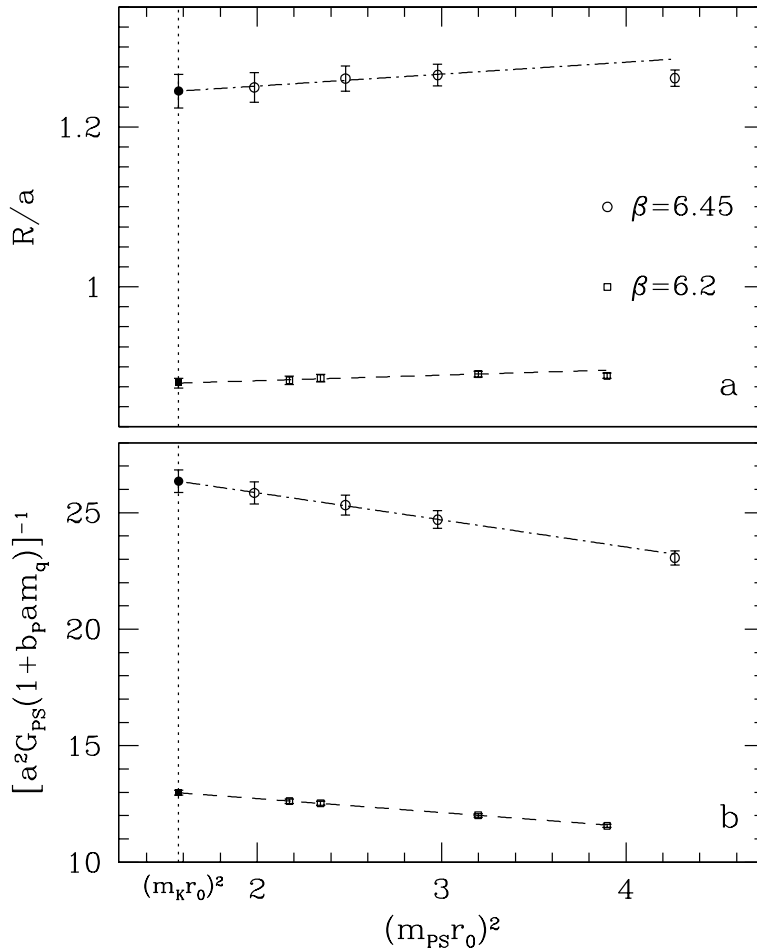


Figure 2: Mass dependence and extrapolations for the two smallest values of the lattice spacing. The ratio R is defined in eq. (A.6).

The second step is now to form the combination

$$r_0(M_s + \hat{M}) = Z_M \frac{R|_{r_0^2 m_{\text{PS}}^2 = 1.5736}}{r_0} \times 1.5736 \quad (5.1)$$

collecting all errors, including the ones on r_0 [47] and the β -dependent one of Z_M [28]. We then extrapolate to the continuum limit linearly in a^2 . As seen in Fig. 3a, the dependence on the lattice spacing is significant – in contrast to the quark mass on smaller volume [48]. As a safeguard against higher order terms in the lattice spacing, we therefore include only the three points with smallest lattice spacing in the extrapolation and obtain our main result

$$r_0(M_s + \hat{M}) = 0.362(12). \quad (5.2)$$

This result contains the β -independent part of the uncertainty in Z_M of 1.3% [28]. At this point one may be concerned about the validity of an a^2 -extrapolation, since $b_A - b_P$ is mostly known only in perturbation theory. However, this combination is found to be tiny at the one-loop level [53] and turns out to be rather small also non-perturbatively [50, 51]. We have checked explicitly that such small values of $b_A - b_P$ do not affect our continuum extrapolation.

In the whole procedure one may replace R , defined in eq. (2.2), by the ratio of the current quark mass and the pseudoscalar mass squared. One then ends up with slightly different lattice spacing effects and somewhat different statistical errors. We have performed also that analysis, using the current quark mass averaged over a range of timeslices around the central one in our lattice. The results differ by up to 2% from the ones presented above for finite lattice spacings but are indistinguishable after the continuum extrapolation.

Instead of the quark mass in units of r_0 , we may also compute the combination $(M_s + \hat{M})/(F_K)_R$, where $(F_K)_R$ is the kaon decay constant. As its experimental value we take $(F_K)_R = 160(2)$ MeV. We note that electromagnetic effects cannot be subtracted in analogy to eq. (1.10), chiefly because F_{K^0} is not known experimentally. We emphasize that this is truly an alternative procedure which amounts to computing the combination

$$\frac{M_s + \hat{M}}{(F_K)_R} = \frac{M}{\bar{m}} \frac{1}{Z_P r_0^2 G_{PS} [1 + b_P a m_q]} \Big|_{r_0^2 m_{PS}^2 = 1.5736} \times 1.5736, \quad (5.3)$$

where the ratio M/\bar{m} and the renormalization constant Z_P have to be taken at a common scale for which we resort to the value $\mu = 1/(1.436r_0)$ chosen in [28]. Discretization effects are clearly expected to be different in this case: they are known to be non-negligible in the product $r_0(F_{PS})_R$ [52]. A non-perturbative estimate being unavailable at present, we have to rely on the perturbative value $b_P = 1 + 0.153 g_0^2$ [53]. Extrapolations in $r_0^2 m_{PS}^2$ and the continuum extrapolations are shown in Fig. 2b and Fig. 3b. Concerning the former, the mass-dependence of $1/\{G_{PS}[1 + b_P a m_q]\}$ is stronger than the mass dependence of R , but within our errors it is perfectly linear and the extrapolation is easily done. In comparison to the quark mass in units of r_0 , we find discretization errors which are roughly only half as big.

In order to confirm that it is legitimate to perform an extrapolation linear in a^2 , even though the improvement coefficient b_P is known only perturbatively, we have repeated the whole analysis after setting b_P to its tree-level value $b_P = 1$. Results after extrapolation changed by much less than a percent. Our final continuum result is

$$\frac{M_s + \hat{M}}{(F_K)_R} = 0.874(29). \quad (5.4)$$

For illustration we may translate to physical units, setting $r_0 = 0.5$ fm [47] and $(F_K)_R = 160(2)$ MeV. We thus obtain

$$M_s + \hat{M} = 143(5) \text{ MeV} \quad \text{from eq. (5.2)}, \quad (5.5)$$

$$M_s + \hat{M} = 140(5) \text{ MeV} \quad \text{from eq. (5.4)}. \quad (5.6)$$

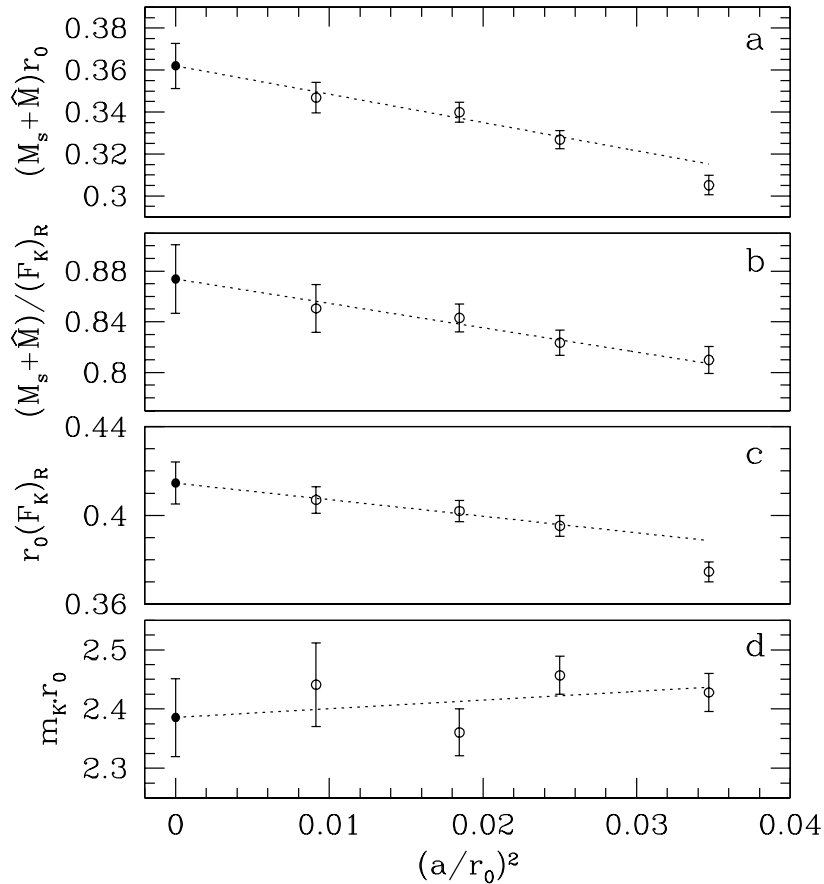


Figure 3: Continuum limit extrapolations of several observables. Full symbols show the extrapolated values. Dashed lines represent the extrapolation function, which are continued outside the fit range towards larger lattice spacings.

As will be discussed in more detail below, this assignment of physical units is ambiguous in the quenched approximation. One should be well aware that the solid results are given in eq. (5.2) and eq. (5.4).

For future reference we list various dimensionless quantities both for $r_0^2 m_{\text{PS}}^2 = 1.5736$ and for $r_0^2 m_{\text{PS}}^2 = 3$ in Table 2. Our results before and after the continuum extrapolation can be found in that table.

6 Ambiguities in the quenched approximation

In the previous section, we have mainly used r_0 as our reference scale. However, in general one expects that by choosing different experimental inputs one will also get somewhat different results when working in the quenched approximation. Here we

would like to quantify this ambiguity for our determination of $M_s + \hat{M}$.

A first estimate is obtained by computing the combination $r_0(F_K)_R$, using our results for the pseudoscalar decay constant including the non-perturbative renormalization factor Z_A , and comparing it to its experimental value. Of course, on the basis of the results for $M_s + \hat{M}$ presented in eqs. (5.5) and (5.6) one may not expect any significant deviation. However, the following detailed analysis may still be instructive, in particular since it yields $r_0(F_K)_R$ in the quenched approximation.

The procedure to extract $r_0(F_K)_R$ is entirely analogous to what was done in the previous section. The extrapolations in $r_0^2 m_{\text{PS}}^2$ (for mass-degenerate quarks) and the continuum extrapolations are shown in Fig. 4a and Fig. 3c, respectively. In the continuum limit we find

$$\text{quenched: } \{r_0 Z_A F_{\text{PS}}[1 + b_A a m_q]\}_{r_0^2 m_{\text{PS}}^2 = 1.5736} = 0.415(9) \quad (6.1)$$

compared to

$$\text{experiment: } 0.5 \text{ fm} \times (F_K)_R = 0.405(5) \quad (6.2)$$

with the experimental value of $(F_K)_R$. Clearly the result obtained in the quenched approximation agrees well with experiment when the approximate value $r_0 = 0.5 \text{ fm}$ is employed. However, it would be premature to conclude that the ambiguity is small, since the agreement may be special to the case of $(F_K)_R$.

Another alternative to set the scale is provided by the nucleon mass, m_N . Compared with other widely used quantities like m_ρ , the nucleon has the advantage of being a stable hadron. Although we have not computed m_N ourselves, we can still use the precise published results obtained by the CP-PACS Collaboration [16] and combine them with the values of r_0/a reported in [47]. We obtain

$$\text{quenched: } r_0 m_N \approx 2.6 \quad (6.3)$$

compared to

$$\text{experiment: } 0.5 \text{ fm} \times m_N = 2.38, \quad (6.4)$$

which represents a 10% difference. Of course also the result for $M_s + \hat{M}$ in MeV would change by the same amount if one used m_N instead of r_0 or $(F_K)_R$ as experimental input. This may serve as a rough estimate of the inherent ambiguity in the quenched model.

In principle one could also use directly the results from recent comparisons of the quenched light hadron spectrum with experiment [16, 54] to estimate this ambiguity. In ref. [16] statistically significant deviations of up to 11% are observed when the scale is set by m_ρ , which, as a resonance, has a fairly large width. Since we consider it safer to set the scale by the nucleon mass, we have refrained from quoting this number as the typical uncertainty for the case at hand. However, using the published numbers

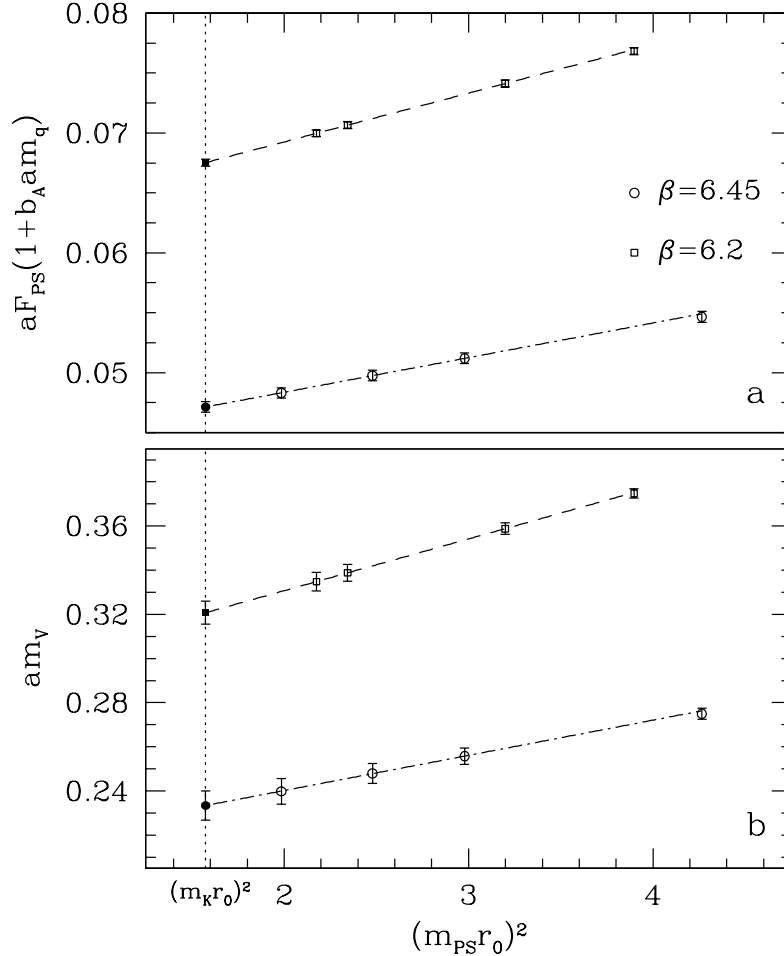


Figure 4: Mass dependence of pseudoscalar decay constant and vector meson mass.

of [16], it is not difficult to estimate the quenched results for the other hadron masses when one chooses m_N as input – at least within a precision of 2-3%. Interestingly it then turns out that the masses of the stable hadrons agree with experiment to within about 4%. On the other hand, for unstable hadrons one observes differences which can be as large as their widths. This may not be too surprising, since resonance effects are not controlled in the lattice calculation. In short, it is difficult to assess the relevance of the deviations observed in the quenched hadron spectrum for our analysis, and thus we stick to our above estimate of around 10% for the ambiguity in question.

Finally, let us discuss the quark mass dependence of the flavour non-singlet vector meson masses in more detail. First we note that effects of the differences of quark masses can be shown to be unimportant in the same way as in Sect. 3 and we restrict our attention to the masses of mass-degenerate mesons ($m_i = m_j$). Our aim is to map out the quark mass dependence of m_V in the continuum limit: we pick certain values of

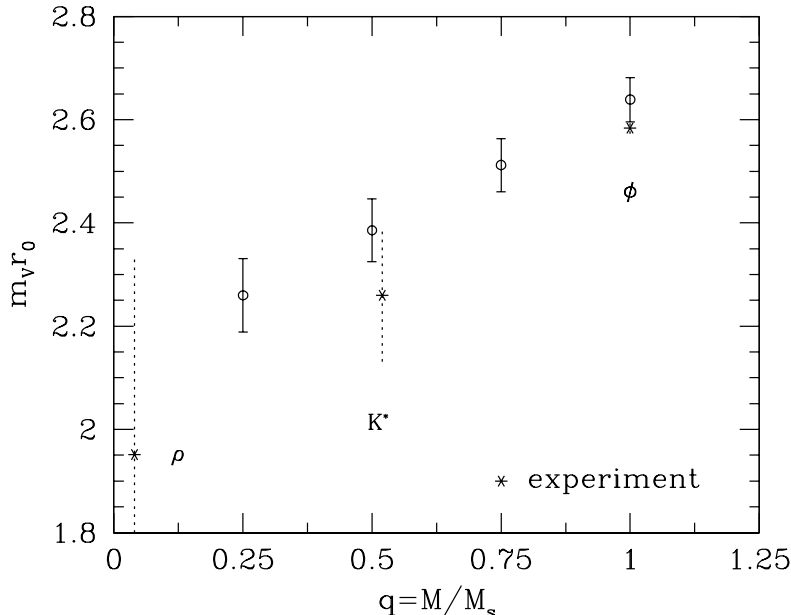


Figure 5: Quark mass dependence of flavour non-singlet vector meson masses. Experimental masses are shown as asterisks and their width is indicated by a dotted line.

$q \equiv m/m_s = M/M_s$, and for each of these values and for each lattice spacing we then perform an inter-/extrapolation of m_V as a function of the quark mass to determine $m_V(m = qm_s)$. Here, $m_s = 1.921 m_{\text{ref}}$ (see eq. (1.1)) is used and m_{ref} is known from the previous section. At fixed value of q we then extrapolate $r_0 m_V$ to the continuum limit including our data for all values of the lattice spacing, after observing that the lattice spacing dependence is very weak.

In Fig. 5, we plot the continuum results as a function of q . They are compared to m_{K^*} , m_ρ and m_ϕ . Since all of these states are resonances, we also indicate their width in the figure. Additional reservations apply to the inclusion of the ϕ meson in this comparison. It is a mixture of flavour octet *and* singlet components, while the lattice calculation is for a pure octet state with mass-degenerate quarks: the disconnected quark diagrams occurring in the singlet channel are not accounted for, and mixing with glueballs is neglected. Although all these effects may be argued to be irrelevant in the quenched approximation, the experimental value in Fig. 5 does include them and it is somewhat surprising that our values for m_V at $q = 1$ come so close to m_ϕ .

If we were to ignore these problems and determined M_s from the requirement that $r_0 m_V$ at that quark mass agrees with $r_0 m_\phi$, it is evident from Fig. 5 that we would obtain a result for M_s which is compatible with the numbers quoted in the previous section. However, the error would be considerably larger. Further continuum results such as $r_0 m_{K^*}$, shown also in Fig. 4b and Fig. 3d, and $(F_K)_R/m_{K^*}$ are listed in Table 2 for future reference.

To summarize, we have directly seen ambiguities of about 10% owing to the use of

the quenched approximation. This has to be kept in mind when quark masses in MeV are quoted. Still we have demonstrated that within the quenched approximation a total precision of 3% (see eq. (5.2) and eq. (5.4)) can be achieved.

7 Discussion

Noting that ratios of light quark masses can at present best be calculated in chiral perturbation theory, we discussed a strategy to compute the overall scale of the light quark masses and applied it to the test-case of quenched QCD.

The problem has essentially two parts. First, the renormalization problem should be solved non-perturbatively. Here we have used the recent solution of the ALPHA-collaboration [28,29] which connects the bare current quark masses to the renormalization group invariant ones. Second, one particular quark mass should be computed by matching with pseudoscalar meson masses. It is not necessary to perform this matching at physical values of the quark masses, because the parameters in the effective chiral Lagrangian are mass-independent. For both the quenched approximation and full QCD it appears convenient to use two different (flavours of) quarks with equal mass M_{ref} such that m_{PS} is equal to the kaon mass m_{K} .

The ratio of M_{ref} to the physical quark masses can then be computed in chiral perturbation theory. In Sect. 3 we have shown that pseudoscalar masses, m_{PS} , have *very little* dependence on the difference of the two quark masses in the quenched approximation. From this one has $2 M_{\text{ref}} \approx M_s + \hat{M}$, which is also true in chiral perturbation theory (in full QCD!).

By making the identification $2M_{\text{ref}} = M_s + \hat{M}$ we have computed $(M_s + \hat{M})r_0$ and $(M_s + \hat{M})/(F_{\text{K}})_{\text{R}}$, incorporating all systematic errors (such as finite size effects), and have taken the continuum limit of these quantities. These solid results are given in eq. (5.2) and eq. (5.4).

A conversion of the results to physical units is necessarily ambiguous, since quenched QCD does not describe the real world. Depending on the choice of quantity somewhat different results in MeV are obtained. It is interesting to note that using either $r_0 = 0.5 \text{ fm}$ or $(F_{\text{K}})_{\text{R}} = 160 \text{ MeV}$ gives indistinguishable results at our level of precision of 3%. However, this does not mean that $M_s + \hat{M}$ has to be very close to our quenched result also in full QCD. Indeed, we have estimated that replacing $(F_{\text{K}})_{\text{R}}$ by m_{N} (or other stable light hadron masses) would give quark masses in MeV, which are larger by about 10%.

Usually the running quark masses in the $\overline{\text{MS}}$ scheme, $\overline{m}_{\overline{\text{MS}}}(\mu)$, are quoted. Their relation to the renormalization group invariant quark masses, which we computed here, has been discussed in Sect. 2 of [28]. For convenience, we include a table with the perturbative conversion factors $\overline{m}_{\overline{\text{MS}}}(\mu)/M$ computed by numerical integration of the renormalization group equations with the n -loop approximations of the renormalization group functions (β, τ in the notation of [28]) for $n = 2, 3, 4$. One should be aware that the result $\Lambda_{\overline{\text{MS}}}^{(0)} = 238(19) \text{ MeV}$ [28] enters the numbers of Table 3. The uncertainty in

μ [GeV]	$\bar{m}_{\overline{\text{MS}}}(\mu)/M$		
	2-loop	3-loop	4-loop
1.0	0.80279	0.83585	0.84449
2.0	0.70388	0.71830	0.72076
4.0	0.64079	0.64880	0.64981
8.0	0.59549	0.60055	0.60105
90.0	0.49937	0.50105	0.50112

Table 3: Factors to convert the renormalization group invariant mass into the $\overline{\text{MS}}$ scheme at scale μ

Λ translates into 1.5% in $\bar{m}_{\overline{\text{MS}}}(\mu)/M$ at $\mu = 2$ GeV and 2.5% at $\mu = 1$ GeV. If desired, Table 3 may be used to estimate $\bar{m}_{\overline{\text{MS}}}(\mu)$. A typical result combining eq. (5.6), eq. (1.1) and the table is

$$\bar{m}_s(2 \text{ GeV}) = 97(4) \text{ MeV} \quad \text{with 4-loop running in the } \overline{\text{MS}} \text{ scheme.} \quad (7.1)$$

This illustrates that a high level of precision can be reached by state of the art lattice techniques.

Effects of dynamical fermions may first be examined in the theory with unphysically large quark masses. We have also given results for a reference mass which is roughly twice the strange quark mass. One should quantify what the effects of dynamical fermions are at such a point, where a good accuracy may be achieved, and then move on to the more chiral regime.

Also for some quantities not related directly to quark masses, precise results have been obtained. They refer to the continuum limit of the quenched approximation and are summarized in Table 2. Most notably, decay constants were computed with a precision not much worse than the experimental one. This was achieved using the method to compute hadronic correlation functions proposed in [43]. In this context we should also comment on the continuum extrapolations in the $O(a)$ improved theory. They are certainly necessary! For the quark mass in units of r_0 , the difference between its value at a lattice spacing $a = 0.1$ fm and at $a = 0$ amounts to about 15%. Other quantities show smaller lattice spacing effects as was observed also in a finite volume study [48]. Although clearly one would have hoped for a weaker a -dependence, we note that their order of magnitude is not much different from what is known already for pure gauge theory observables [47].

Finally let us come back to the rôle of lattice QCD in determining parameters of the chiral Lagrangian. Figs. 2 and 4a show to what precision the quark mass dependence of observables in the pseudoscalar sector can be computed. Such information, once available in full QCD, will allow to reduce the errors in the chiral Lagrangian. For instance, we have checked that just the mass independence of R puts strong restrictions

on these parameters. As usual, estimates of the uncertainties is a delicate issue and a detailed investigation of the potential of this approach will be left for future work.

The project of computing light quark masses was started quite a while ago by the ALPHA collaboration. Here we presented the final results. The basis of our approach was developed together with M. Lüscher, S. Sint and P. Weisz. We would like to thank them for a most enjoyable collaboration. In particular, R.S. and H.W. thank M. Lüscher for numerous enlightening discussions. Furthermore, we appreciate useful correspondence with G. Ecker and D. Wyler on chiral perturbation theory and electromagnetic corrections.

The numerical computations were performed on the APE100/Quadrics computers of DESY Zeuthen and on the Cray T3D at EPCC Edinburgh. We thank these institutions for their support. This work was in part supported by EPSRC grant GR/K41663 and PPARC grants GR/K55745 and GR/L29927.

A Numerical details

A.1 Improvement coefficients, renormalization factors

Our calculations have been performed using the $O(a)$ improved Wilson action defined in ref. [37], which can be consulted for any unexplained notation. In particular, the improvement coefficients c_{sw} and c_A were taken from eqs. (5.15) and (6.4) of that reference.

The renormalized axial current and pseudoscalar density for quark flavours i and j are defined as

$$(A_R)_\mu(x) = Z_A(1 + b_A am_q)(A_I)_\mu(x), \quad (\text{A.1})$$

$$P_R(x) = Z_P(1 + b_P am_q)P(x), \quad (\text{A.2})$$

where $P(x) = \bar{\psi}_i(x)\gamma_5\psi_j(x)$, and the improved, unrenormalized axial current is given by

$$(A_I)_\mu(x) = \bar{\psi}_i(x)\gamma_\mu\gamma_5\psi_j(x) + ac_A\frac{1}{2}(\partial_\mu^* + \partial_\mu)P(x). \quad (\text{A.3})$$

The renormalization factor Z_A was calculated in [49], and here we have used its parameterization in eq. (6.11) of that paper.

The renormalization factor Z_M , which relates the current quark mass in the $O(a)$ improved theory to the renormalization group invariant quark mass, has recently been determined [28]. In that paper also the scale- and scheme-dependent factor Z_P has been computed in the Schrödinger functional (SF) scheme at a fixed scale of $L = 1.436 r_0$. Here we use their representation in terms of polynomial fit functions, viz.

$$Z_M(g_0) = 1.752 + 0.321(\beta - 6) - 0.220(\beta - 6)^2, \quad (\text{A.4})$$

$$Z_P(g_0, L/a)_{L=1.436 r_0} = 0.5233 - 0.0362(\beta - 6) + 0.0430(\beta - 6)^2, \quad (\text{A.5})$$

$$\beta = 6/g_0^2, \quad 6.0 \leq \beta \leq 6.5.$$

As explained in Subsect. 6.2 of ref. [28], the uncertainty in Z_M is split into a β -dependent part of 1.1%, which enters any continuum extrapolation, and a β -independent error of 1.3% which must be added (in quadrature) to the extrapolated result. The typical accuracy of Z_P as given by the above polynomial is 0.5%.

The factor Z_M renormalizes the lattice counterpart of the ratio $R(m_i, m_j)$ defined in eq. (2.1). In the $O(a)$ improved theory it is given by

$$R(m_i, m_j) = \frac{F_{\text{PS}}}{G_{\text{PS}}} [1 + (b_A - b_P)am_q], \quad (\text{A.6})$$

where

$$m_q = \frac{1}{2} \{ (m_q)_i + (m_q)_j \} = \frac{1}{4a} \left(\frac{1}{\kappa_i} + \frac{1}{\kappa_j} - \frac{2}{\kappa_c} \right), \quad (\text{A.7})$$

and κ_i, κ_j are the hopping parameters of flavours i and j .

The combination $b_A - b_P$ has been found to be small in perturbation theory [53] and also non-perturbatively [50, 51]. A method how to determine the individual coefficients b_A and b_P non-perturbatively has been proposed in ref. [55], but no results for our choice of action have been reported so far.

The values for the critical hopping parameter κ_c have been taken from Table 1 of ref. [37]. When necessary they have been interpolated linearly to the desired β -value.

A.2 Hadronic correlation functions, reference scale

Our calculation of hadronic correlation functions using Schrödinger functional boundary conditions follows exactly the procedures outlined in a previous paper [43]. In particular, this reference contains the definitions of the correlation functions f_P, f_A^I, k_V^I and f_1 , which we have computed to extract hadron masses and matrix elements for pseudoscalar and vector mesons.

Estimates for meson masses were obtained by averaging effective masses,

$$am_{\text{eff},X}(x_0 + \frac{a}{2}) = \ln(f(x_0)/f(x_0 + a)), \quad X = \text{PS}, \text{V}, \quad (\text{A.8})$$

over a suitably chosen interval $t_{\min} \leq x_0 \leq t_{\max}$. Similarly, the ratio $F_{\text{PS}}/G_{\text{PS}}$ was obtained by averaging the combination

$$\frac{F_{\text{PS}}}{G_{\text{PS}}} = \frac{1}{m_{\text{PS}}} \frac{f_A^I(x_0)}{f_P(x_0)}, \quad (\text{A.9})$$

and the individual matrix elements F_{PS} and G_{PS} are extracted from

$$F_{\text{PS}} = 2(m_{\text{PS}} L^3)^{-1/2} e^{(x_0 - T/2)m_{\text{PS}}} \frac{f_A^I(x_0)}{\sqrt{f_1}}, \quad (\text{A.10})$$

$$G_{\text{PS}} = 2(m_{\text{PS}}/L^3)^{1/2} e^{(x_0 - T/2)m_{\text{PS}}} \frac{f_P(x_0)}{\sqrt{f_1}}, \quad (\text{A.11})$$

where again an average over the interval $[t_{\min}, t_{\max}]$ is taken. The averaging intervals used here were the same as those in Table 1 of ref. [43].

We have also calculated an unrenormalized current quark mass defined by

$$m(x_0) = \frac{\frac{1}{2}(\partial_0^* + \partial_0)f_A(x_0) + c_A a \partial_0^* \partial_0 f_P(x_0)}{2f_P(x_0)}. \quad (\text{A.12})$$

The values for the current quark mass listed in Table 1 have been obtained by averaging $m(x_0)$ over the interval $T/4 \leq x_0 \leq 3T/4$.

For the hadronic radius r_0 which was used to set the scale, we have taken its parameterization quoted in [47], viz.

$$\ln(a/r_0) = -1.6805 - 1.7139(\beta - 6) + 0.8155(\beta - 6)^2 - 0.6667(\beta - 6)^3, \quad (\text{A.13})$$

accounting for the uncertainty as quoted in [47]. In addition to the results obtained at $\beta = 6.0$ and 6.2 , which have been published in [43], we have also computed correlation functions at $\beta = 6.1$ and 6.45 . A brief summary of our simulation parameters including N_{meas} , the number of gauge field configurations for which the correlation functions were computed, is presented in Table 4.

β	T/a	L/a	L/r_0	N_{meas}
6.0	32	16	2.981(12)	1000
6.1	40	24	3.795(17)	800
6.2	48	24	3.261(16)	800
6.45	64	32	3.060(17)	220

Table 4: Simulation parameters

References

- [1] J. Gasser and H. Leutwyler, Phys. Rept. 87 (1982) 77.
- [2] H. Leutwyler, (1994), hep-ph/9406283.
- [3] H. Leutwyler, Phys. Lett. B378 (1996) 313, hep-ph/9602366.
- [4] C.R. Allton et al., Nucl. Phys. B431 (1994) 667, hep-ph/9406263.
- [5] C.R. Allton, V. Giménez, L. Giusti and F. Rapuano, Nucl. Phys. B489 (1997) 427, hep-lat/9611021.
- [6] V. Giménez, L. Giusti, F. Rapuano and M. Talevi, Nucl. Phys. B540 (1999) 472, hep-lat/9801028; L. Giusti, V. Giménez, F. Rapuano, M. Talevi and A. Vladikas, (1998), hep-lat/9809037.

- [7] UKQCD Collaboration, C.R. Allton et al., Phys. Rev. D49 (1994) 474, hep-lat/9309002.
- [8] R. Gupta and T. Bhattacharya, Phys. Rev. D55 (1997) 7203, hep-lat/9605039.
- [9] B.J. Gough, G.M. Hockney, A.X. El-Khadra, A.S. Kronfeld, P.B. Mackenzie, B.P. Mertens, T. Onogi and J.N. Simone, Phys. Rev. Lett. 79 (1997) 1622, hep-ph/9610223.
- [10] M. Göckeler, R. Horsley, H. Perlt, P. Rakow, G. Schierholz, A. Schiller and P. Stephenson, Phys. Rev. D57 (1997) 5562, hep-lat/9707021.
- [11] A. Cucchieri, M. Masetti, T. Mendes and R. Petronzio, Phys. Lett. B422 (1998) 212, hep-lat/9711040; A. Cucchieri, T. Mendes and R. Petronzio, J. High Energy Phys. 05 (1998) 006, hep-lat/9804007.
- [12] D. Becirevic, Ph. Boucaud, J.P. Leroy, V. Lubicz, G. Martinelli and F. Mescia, Phys. Lett. B444 (1998) 401, hep-lat/9807046.
- [13] SESAM Collaboration, N. Eicker et al., Phys. Lett. B407 (1997) 290, hep-lat/9704019; SESAM Collaboration, N. Eicker et al., Phys. Rev. D59 (1999) 014509, hep-lat/9806027.
- [14] T. Blum, A. Soni and M. Wingate, (1999), hep-lat/9902016.
- [15] JLQCD Collaboration, S. Aoki et al., Phys. Rev. Lett. 82 (1999) 4392, hep-lat/9901019.
- [16] CP-PACS Collaboration, S. Aoki et al., (1999), hep-lat/9902018.
- [17] J. Bijnens, J. Prades and E. de Rafael, Phys. Lett. B348 (1995) 226, hep-ph/9411285.
- [18] M. Jamin and M. Münz, Z. Phys. C66 (1995) 633, hep-ph/9409335.
- [19] M. Jamin, Nucl. Phys. B (Proc. Suppl.) 64 (1998) 250, hep-ph/9709484.
- [20] S. Narison, Phys. Lett. B358 (1995) 113, hep-ph/9504333.
- [21] K.G. Chetyrkin, D. Pirjol and K. Schilcher, Phys. Lett. B404 (1997) 337, hep-ph/9612394.
- [22] P. Colangelo, F.D. Fazio, G. Nardulli and N. Paver, Phys. Lett. B408 (1997) 340, hep-ph/9704249.
- [23] J. Prades, Nucl. Phys. B (Proc. Suppl.) 64 (1998) 253, hep-ph/9708395.
- [24] F.J. Ynduráin, Nucl. Phys. B517 (1998) 324, hep-ph/9708300.

- [25] H.G. Dosch and S. Narison, Phys. Lett. B417 (1998) 173, hep-ph/9709215.
- [26] L. Lellouch, E. de Rafael and J. Taron, Phys. Lett. B414 (1997) 195, hep-ph/9707523.
- [27] K. Maltman, (1999), hep-ph/9904370.
- [28] ALPHA Collaboration, S. Capitani, M. Lüscher, R. Sommer and H. Wittig, Nucl. Phys. B544 (1999) 669, hep-lat/9810063.
- [29] ALPHA Collaboration, S. Sint and P. Weisz, Nucl. Phys. B545 (1999) 529, hep-lat/9808013.
- [30] R. Dashen, Phys. Rev. 183 (1969) 1245.
- [31] K. Maltman and D. Kotchan, Mod. Phys. Lett. A5 (1990) 2457; J.F. Donoghue, B.R. Holstein and D. Wyler, Phys. Rev. D47 (1993) 2089; J. Bijnens, Phys. Lett. B306 (1993) 343, hep-ph/9302217; R. Baur and R. Urech, Phys. Rev. D53 (1996) 6552, hep-ph/9508393; J.F. Donoghue, private communication through D. Wyler.
- [32] R. Sommer, Nucl. Phys. B411 (1994) 839, hep-lat/9310022.
- [33] J. Gasser and H. Leutwyler, Ann. Phys. 158 (1984) 142.
- [34] J. Gasser and H. Leutwyler, Nucl. Phys. B250 (1985) 465.
- [35] J. Bijnens, G. Ecker and J. Gasser, (1994), hep-ph/9411232.
- [36] M. Lüscher, S. Sint, R. Sommer and P. Weisz, Nucl. Phys. B478 (1996) 365, hep-lat/9605038.
- [37] M. Lüscher, S. Sint, R. Sommer, P. Weisz and U. Wolff, Nucl. Phys. B491 (1997) 323, hep-lat/9609035.
- [38] S.R. Sharpe, Phys. Rev. D41 (1990) 3233; J.N. Labrenz and S.R. Sharpe, Phys. Rev. D54 (1996) 4595, hep-lat/9605034.
- [39] C.W. Bernard and M.F.L. Golterman, Phys. Rev. D46 (1992) 853, hep-lat/9204007; Nucl. Phys. B (Proc. Suppl.) 30 (1993) 217.
- [40] M. Booth, G. Chiladze and A.F. Falk, Phys. Rev. D55 (1997) 3092, hep-ph/9610532.
- [41] W. Bardeen, A. Duncan, E. Eichten, G. Hockney and H. Thacker, Phys. Rev. D57 (1998) 1633, hep-lat/9705008.
- [42] UKQCD Collaboration, K.C. Bowler et al., Quenched QCD with $O(a)$ improvement: 'I. The spectrum of light hadrons', in preparation.

- [43] ALPHA Collaboration, M. Guagnelli, J. Heitger, R. Sommer and H. Wittig, (1999), hep-lat/9903040.
- [44] J. Gasser and H. Leutwyler, Phys. Lett. 184B (1987) 83.
- [45] M. Lüscher, Lectures given at Summer School 'Fields, Strings and Critical Phenomena', Les Houches, France, Jun 28 - Aug 5, 1988.
- [46] M. Lüscher, Commun. Math. Phys. 104 (1986) 177.
- [47] ALPHA Collaboration, M. Guagnelli, R. Sommer and H. Wittig, Nucl. Phys. B535 (1998) 389, hep-lat/9806005.
- [48] ALPHA Collaboration, J. Heitger, (1999), hep-lat/9903016.
- [49] M. Lüscher, S. Sint, R. Sommer and H. Wittig, Nucl. Phys. B491 (1997) 344, hep-lat/9611015.
- [50] G.M. de Divitiis and R. Petronzio, Phys. Lett. B419 (1998) 311, hep-lat/9710071.
- [51] T. Vergata and ALPHA Collaborations, work in progress.
- [52] H. Wittig, Nucl. Phys. B (Proc. Suppl.) 63 (1998) 47, hep-lat/9710013.
- [53] S. Sint and P. Weisz, Nucl. Phys. B502 (1997) 251, hep-lat/9704001.
- [54] F. Butler, H. Chen, J. Sexton, A. Vaccarino and D. Weingarten, Nucl. Phys. B430 (1994) 179, hep-lat/9405003.
- [55] T. Bhattacharya, S. Chandrasekharan, R. Gupta, W. Lee and S. Sharpe, (1999), hep-lat/9904011.